

Numerical Modeling of Passive Loaded Raked Pile Group in Multilayered Soil

Yasmin.M.Nady, Fayek Hassona, Ahmed Mousa, Beshoy M. Hakeem

Department of Civil Engineering, Faculty of Engineering, Nahda University, Beni Suef 0822284688, Egypt
Department of Civil Engineering, Faculty of Engineering, Minia University, 61519 Minia, Egypt
Department of Civil engineering, Higher Institute of Engineering and Technology New Minia, Egypt

ABSTRACT

Piles that support bridge abutments resting on soft clay are exposed to horizontal loads caused by the lateral displacement of the soil induced by an adjacent embankment. Raked piles are known for their effectiveness in resisting active lateral loads. However, their performance under passive loading conditions remains a subject of debate and requires further investigation. In this study, a numerical study was conducted to explore the effect of using a single row of raked piles (RPG) under a bridge abutment on soft clay soil and compared it with a vertical pile group (VPG) using PLAXIS 3D (v21). The study considered various factors, including the inclination angle, and embankment load. The results from FEM analyses indicated that, an increase in embankment stress causes higher lateral pile displacement, maximum bending moment, and lateral pressure. Increasing inclination angle of the pile produces lower lateral movements and bending moment however, an increase in the pile inclination angle may cause damage to the structural system. A typical angle of 10 degrees for raked piles showed good behavior

Keywords: Soft clay, Passive piles, Pile-soil interaction, Embankments, raked pile

INTRODUCTION

Piles are designed to resist axial loads from the superstructure by utilizing shaft friction and/or end bearing, both of which are a result of movement between the pile and the surrounding soil. When a pile faces a lateral load, which can be either static or cyclic, it is supported laterally by the soil (i.e., active piles). The extent of lateral displacement of the pile, as well as the resulting flexural moment, is influenced by several factors. These include the relative density of the soil (in the case of coarse-grained soils), the undrained cohesive strength (in fine-grained soils), the comparative stiffness of the pile and soil, the eccentricity of the load, the inclination of the piles, and the condition of the pile head (Rao et al. 1996, Karthigeyan et al. 2007, Basack and Dey 2012, Abbas et al. 2018).

However, the consolidation of soft soils can also impose additional loads on piles, either axially (known as dragload, as discussed in studies by Comodromos and Bareka 2005, Fellenius 2006, Hanna and Sharif 2006, El-Mossallamy et al. 2013, Morsy 2013) or laterally, due to increased lateral pressure from the movement of adjacent consolidating soil (as explored in research by Poulos 1973, Springman 1989, Jeong et al. 2004, Li et al. 2019). These scenarios involve passive piles, which are typically found in soft soils under certain conditions. Such piles, known as passive piles, are typically found in soft soils under certain conditions. Passive piles are commonly used in scenarios like supporting bridge abutments near bridge approaches, stabilizing slopes, and piles located close to excavations for deep basements or near tunneling activities (Loganathan et al. 2000, Zhao et al. 2008, Kahyaoglu et al. 2009, Karim 2013, Guo 2016, Bellezza and Caferri 2018, Soomro et al. 2019, Zhang et al. 2020)

When constructing bridge abutments on consolidating soft soil, it's crucial to design the supporting piles as passive piles. This is because the stress from the bridge approach can lead to lateral compression of the soft soil beneath, resulting in lateral soil movement. Such movement can cause additional lateral displacement of the pile and associated bending moments, as noted in AASHTO 2017. Therefore, it's vital to account for this extra lateral pile displacement and bending moment to prevent structural failure of the pile section or serviceability issues, as highlighted in studies by Moulton et al. 1985, Pan et al. 2002, Jones et al. 2008, and Zhao et al. 2008.

The efficacy of passive piles has been extensively investigated through both experimental testing and numerical modeling. Centrifuge tests were conducted to understand the behavior of passive piles, and subsequently used to develop empirical design methods (Oteo 1977, Springman 1989, Stewart 1992, Ellis 1997, Jeong et al. 2004). The main outcomes from these centrifuge tests revealed that the maximum lateral pile displacement and bending moment typically occur at the pile head. Furthermore, it was observed that the lateral displacement of both the rear piles (those farthest from the bridge approach embankment) and the front piles (those closest to the bridge approach embankment) was comparable. However, the rear piles experienced a higher bending moment compared to the front piles.

Additionally, the bending moments and lateral displacements of piles were increased over time as a result of the consolidation of the soft layer and the dissipation of excess pore-water pressure. This was coupled with a gradual decrease in passive loading on the rear pile. The outcomes of these centrifuge tests were further examined through back-analysis using numerical finite-element modeling. This modeling involved either employing a plane strain model to represent the row of piles as a sheet pile wall with equivalent bending stiffness or using a three-dimensional mode (Springman 1989, Bransby and Springman 1996, Stewart et al.

1996, Ellis and Springman 2001, and Kelesoglu and Springman 2011). The lateral pile displacement predicted through numerical modeling was found to either underestimate or closely align with the results obtained from centrifuge tests.

Numerical modeling has been used to investigate various factors that might affect the performance of passive piles. These factors encompass the construction sequence, the relative stiffness between the pile and soil, and the configuration of the pile group. Studies by Yang et al. (2017) and Alabboodi and Sabbagh (2019) found that a higher pile-soil relative stiffness or a slower application of load leads to reduced displacement at the pile head. Additionally, the lateral earth pressure effect on the row of piles closest to an adjacent surcharge was higher than that on other rows (Zhao et al. 2008). Another aspect impacting passive pile capacity is soil contamination adjacent to the pile, specifically with fuel oil, as highlighted by Karkush and Kareem (2021). Such contamination can decrease soil strength and increase its compressibility, leading to greater lateral pile displacement and maximum bending moment. However, studies examining the impact of the pile's angle of inclination on its capacity and performance underneath the embankment are yet to be conducted.

Designing a piled bridge abutment on soft clay poses a challenge for geotechnical engineers due to the high compressibility, low strength, and low permeability of the clay layer. Soil movement induced by the embankment supported by the abutment results in negative loading on the piles, leading to an increase in bending moment and pile displacement. This, in turn, escalates the risk of structural failure, particularly when a layer of soft clay overlays a stiff layer. The consolidation and creep performance of the soft clay further complicates the problem, introducing time-dependent behavior. This is reflected in the vertical and lateral deformations of the soft layer, which increase the bending moment and lateral displacement of the passive piles. Before the soil begins to move, the soil surrounding the pile is in equilibrium at any depth under the initial stress state. However, as the soil starts to move, the stress in the soil surrounding the pile shifts from its initial state to a new equilibrium. This results in the development of lateral forces on the raked pile shafts, leading to increased pile bending moments and deflections (Miao et al., 2006). Raked piles subjected to such loading have not been extensively studied, and further research is needed. Zhou et al. (2023) pointed out that the performance of passive raked piles in resisting lateral soil movement induced by the embankment has not received sufficient attention to date.

Thus, in view of the paucity of research investigating the raked pile performance underneath embankments, the objective of this paper is to:

1. Examine the behavior of both vertically installed and raked passively loaded piles.
2. Investigate the performance of piles within bridge abutments founded on soft clay, a scenario that leads to passive loading on the piles. Utilize the proposed model, which presents a complex challenge in geotechnical engineering, to conduct this study.
3. Explore the impact of employing a row of raked piles in bridge abutments supported on piles, considering various raking angles. Analyze the factors affected by the raking angle in detail.
4. Conduct a parametric and comparative analysis of both vertical and raked pile groups, considering multiple parameters such as the raked pile's inclination angle, and embankment load.

1. NUMERICAL MODELLING

1.1 Case study

Ellis (1997) conducted a series of centrifuge tests to examine the behavior of a passively loaded pile group installed in a multilayered subsoil. The fundamental principle behind centrifuge testing is to simulate real-life stress conditions on a reduced scale. In these tests, dimensions and time are scaled down by factors of $(1/n)$ and $(1/n^2)$ respectively (Taylor 2018). The centrifuge test setup by Ellis (1997) included a rigid box containing multi-layered soil, abutment, piles, and a pile cap. This setup contains a 100 mm-thick layer of soft kaolin clay above a 100 mm-thick sandy layer, both located below the groundwater table. Six piles, penetrating through the soft clay and resting on the sandy layer, were installed. These piles, made of aluminum, were 12.7 mm in diameter and 190 mm in length. They were rigidly attached at the top to prevent movement and rotation, secured by a 10 mm-thick aluminum pile cap. An 80 mm-high embankment, simulating a bridge approach, was placed atop the soft soil to apply the load.

1.2 Numerical modeling

1.2.1 Validation model

1.2.1.1 Validation model (Model configuration)

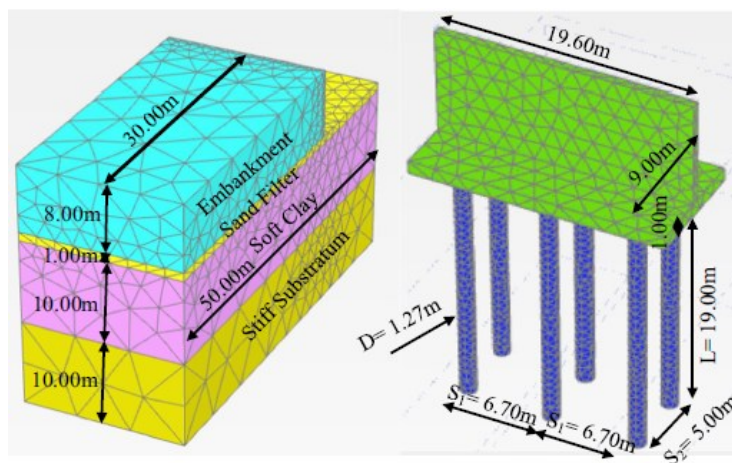
The selected model's dimensions were specified as 19.6 m along the X-axis and 50 m along the Y-axis to avoid boundary effect (Figure 1; Abo-Youssef et al. 2021). In the Z-axis, the boundaries were defined by the embankment height at 8m for the upper boundary and the base of the substratum for the lower boundary. The vertical boundaries of the numerical model were adjusted to allow vertical settlement while limiting the horizontal displacement of the soil layers. The hydraulic boundary conditions assigned allow water to drain through the horizontal boundaries while being restricted through the vertical boundaries. The finite element mesh was composed of ten-noded tetrahedral elements, with the mesh size being finer near the structural elements and coarser at the model's boundaries to reduce the time required for solving the model.

(Table 1) shows the soil parameters used in the validation. The elastoviscoplastic Soft Soil Creep constitutive model, integrated into PLAXIS 3D, was utilized to simulate the soft soil layer, enabling the estimation of deformations due to primary consolidation and secondary compression. Meanwhile, the embankment and the stiff sandy substratum were represented using the double-hardening constitutive soil model. Structural components, including the piles, pile cap, and abutment, were modeled using linear elastic volume elements. This model is a nonlinear elastoplastic, incorporating shear hardening to depict plastic shear strain under deviatoric loading and compression hardening for modeling plastic volumetric strain in primary compression. In the Hardening Soil Model, soil stiffness is dependent on the magnitude of stress and is further influenced by loading, unloading, and reloading cycles (Schanz et al. 1999). Soil stiffness within this model is characterized by three key stiffness parameters, representing different stress paths: triaxial loading stiffness (E_{50}), triaxial unloading-reloading stiffness (E_{ur}), and the oedometer loading modulus (E_{oed}).

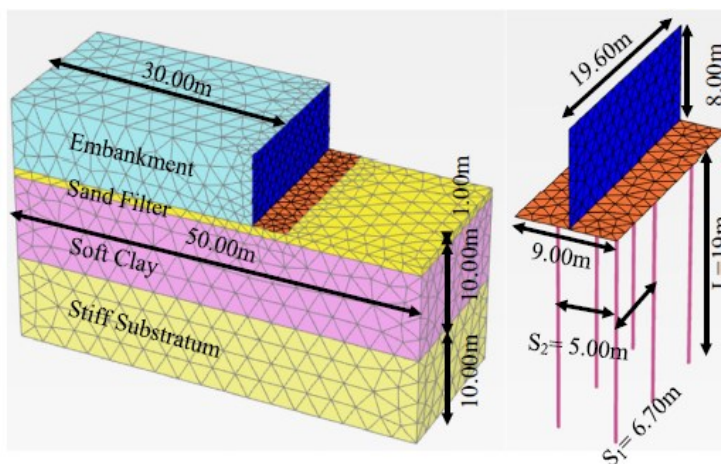
The numerical model was designed to simulate the stages of construction of piles supporting an abutment and an adjacent embankment. This approach allowed for the gradual dissipation of excess pore water pressure, the progressive strengthening of the soft soil layer, and changes in deformation parameters over time, all of which were considered through consolidation analysis.

The model's results were compared to the same measured from centrifuge tests and findings reported by Abo-Youssef et al. (2021) for the same consolidation time. The consolidation analysis estimated soil lateral movement and pile displacement after 21 days post-embankment construction and after 1000 days, representing a long-term period after construction (indicating a 90% degree of consolidation).

The piles were simulated in the validation model using the volume element (approach 1) Table2, and structural element (approach 2) as shown in Figure 1.



(a) Simulated structural elements using Approach1



(b) Simulated structural elements using Approach2

Figure 1. Goemerty and finite element mesh of Approach 1 (piles, pile cap, and abutment were simulated by volume elements) and Approach2 (piles, pile cap and abutment were simulated using beam element) (Abo-Youssef et al. (2021))

Table 1. Soil parameters used in the finite element analyses (Abo-Youssef et al. 2021)

Soil Type	Soft Clay	Embankment	Sand Filter & Sand Substratum
Soil Model	Soft Soil Creep (SSC)	Hardening soil (HS)	Hardening soil (HS)
Drainage Type	Undrained (A)	Drained	Drained
γ_{unsat} (KN/m ³)	14.00	17.00	19.00
γ_{sat} (KN/m ³)	16.50	17.50	19.50
e_{int}	1.33	0.5	0.67
C_c	0.43	----	----
C_s	0.07	----	----
C_α	0.00635	----	----
E_{50}^{ref} (KPa)	----	11,000	25,000
E_{oed}^{ref} (KPa)	----	11,000	25,000
E_{ur}^{ref} (KPa)	----	33,000	75,000
Stress Power (m)	----	0.5	0.5
C' (kPa)	1	1	1
ϕ' (degree)	23	35	35
v_{ur}	0.15	0.2	0.2
v'	----	----	----
$K_{o_{nc}}$	0.69	0.43	0.43
K_x (m/day)	2.29×10^{-4}	0.86	0.86
K_y (m/day)	2.29×10^{-4}	0.86	0.86
K_z (m/day)	1.149×10^{-4}	0.86	0.86
OCR	1	----	----

Table 2. Material parameters of structural elements used in the finite element model conducted using Volume elements (Approach 1). (Abo-Youssef et al. 2021)

Structural Element	Abutment wall	Pile Cap	Pile
Constitutive Model	Linear Elastic (LE)	Linear Elastic (LE)	Linear Elastic (LE)
Drainage Type	Non-Porous	Non-Porous	Non-Porous
γ (KN/m ³)	27	27	27
E (KN/ m ²)	70×10^6	70×10^6	70×10^6
ν	0.15	0.15	0.15

1.2.1.2 Validation model (Results and discussions)

Figure 2, Figure 3, and Table 3, summarized the comparison between the finite element model with the centrifuge results and Abo-Youssef et al. (2021) analysis. Lateral displacement for front pile in current analysis using volume pile and embedded pile was underestimated the centrifuge test however analysis by Abo-Youssef et al. (2021) was overestimated using embedded pile .For the current analysis using embedded pile gave more accurate results for lateral displacement of piles, probably changing value of interface reduction factor (Rinter) in volume piles give more accurate results as this factor had effective effect in the analysis as discussed by (Dao, 2011).Good agreement was obtained for current validation and Abo-Youssef et al. (2021)

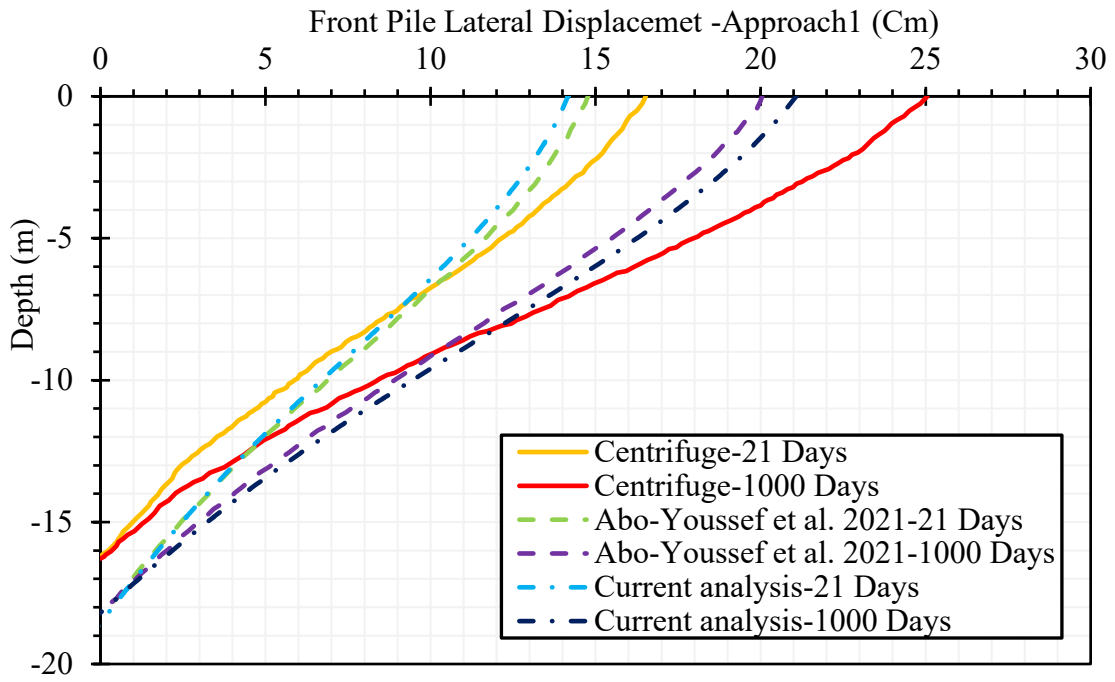


Figure 2. Lateral displacement for front pile for 21 days and 1000 days using (Approach1; volume element)

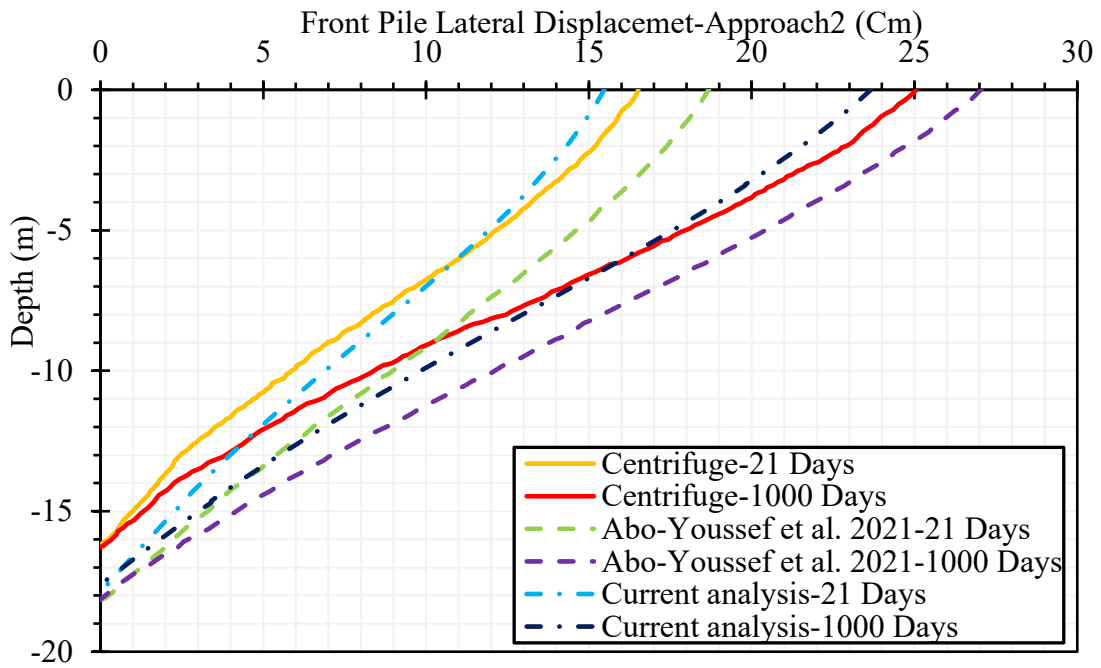


Figure 3. Lateral displacement for front pile for 21 days and 1000 days using (Approach2; structural element)

Table 3. Summarized results of lateral displacement of front pile

Study Type		centrifuge	A. Abo-Youssef (2021)	Current 3D FEM study	%Difference (Centrifuge test & Current study)	%Difference (A. Abo-Youssef (2021) & Current study)
Max. Lateral Displacement (21Days) (Cm)	Approach1	16	14.75	14.16	-11.5 %	- 4.0%
	Approach2		18.7	15.47	-3.31 %	- 17.27 %
Max. Lateral Displacement (1000Days) (Cm)	Approach1	25	20.5	21.07	-15.72 %	+2.78%
	Approach2		27.05	23.66	-5.36 %	-12.53 %

1.2.2 Parametric study

The same validation model was used to examine the effect of the inclination of the piles. The model used only embedded beam elements and plate elements to simulate the piles and structure elements. A pile group featuring rear pile rows at varying raking angles was utilized (referred to as RPG). In all the models, the front row of piles was vertical, while the rear row was set at different raking angles, as illustrated in Figure 4. The changing of inclination angles (7.5°, 10°, 15°, 20°, 30°) were examined, while keeping parameters constant (i.e., embankment load at 140 KPa and the duration of embankment construction at 21 days), was examined.

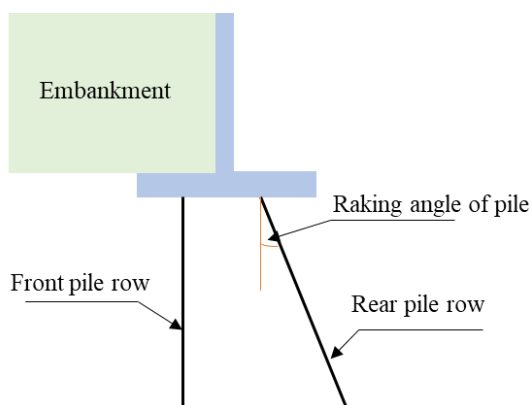


Figure 4. Configuration of the model for the raked pile group

1.2.2.1 Lateral Deformation of Soft Clay Layer

The lateral movement of the soft clay layer decreased with an increase in the raking angle of the rear pile (Figure 5). For the vertically piled group (VPG), the lateral movement of soft clay was 54.25 cm, which then decreased to 46.31, 46.16, 43.78, 41.91, and 40.41 cm for rear piles with raking angles of 7.5°, 10°, 15°, 20°, and 30°, respectively. These reductions correspond to decreases of 14.64%, 14.91%, 19.30%, 22.75%, and 25.59% in comparison to the lateral movement observed in the case of a vertical rear pile. This reduction is attributed to the reverse lateral movement of the entire system due to the inclination of the piles.

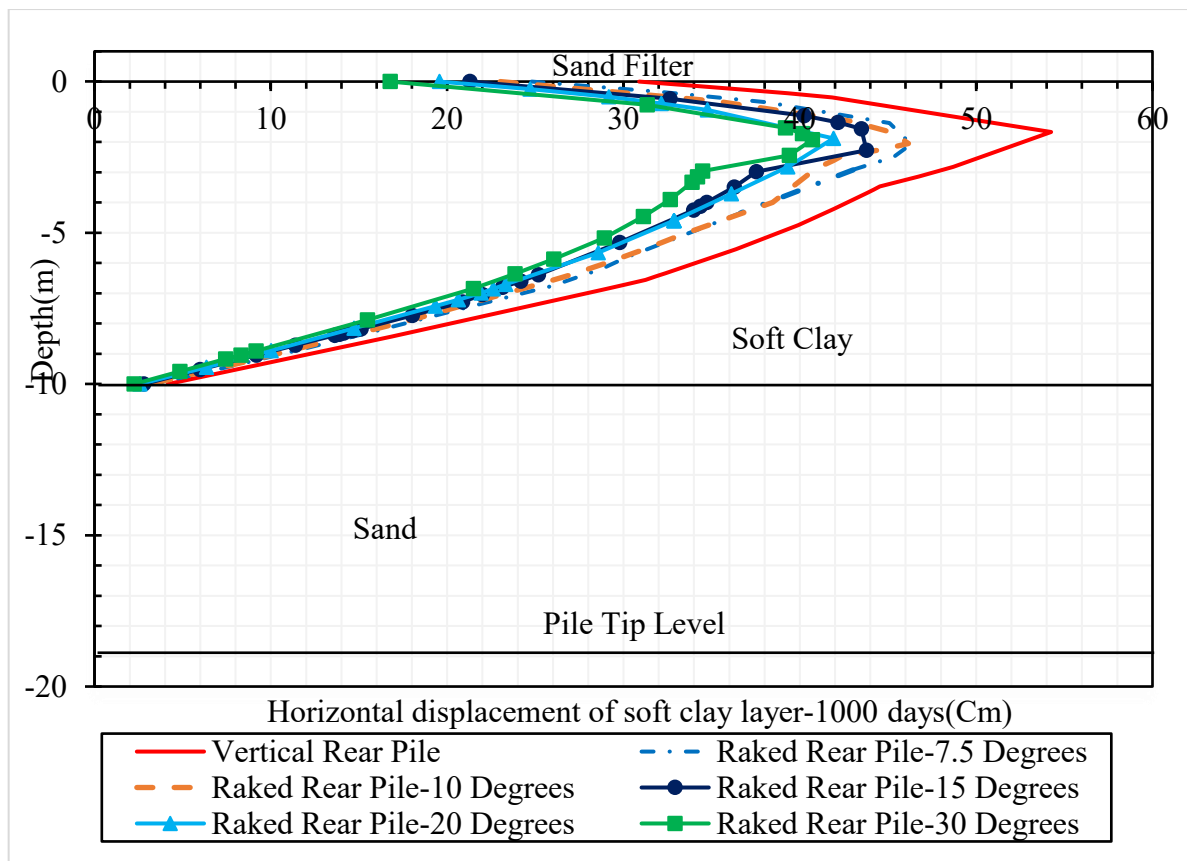


Figure 5. Lateral movement of soft clay layer using different raking angles for rear pile row for 1000 days

1.2.2.2 Lateral Load Per Unit Length for Front and Rear Pile

While the lateral movement of the soft clay layer was reduced, the passive loading on the front pile increased by percentages of 12.92%, 14.66%, 25.64%, 20.21%, and 32.06% for rear piles with raking angles of 7.5°, 10°, 15°, 20°, and 30°, respectively, compared to the case with a vertical rear pile, as illustrated in Figure 6. This increase in passive loading is attributed to the reverse movement of the front pile towards the embankment, which generated greater resistance from the soil against the pile. Consequently, the active loading on the sand layer saw a reduction by 23.30%, 40.15%, 46.00%, 40.03%, and 68.40% for the respective raking angles of 7.5°, 10°, 15°, 20°, and 30°, compared to the active loading in the scenario of a vertical rear pile.

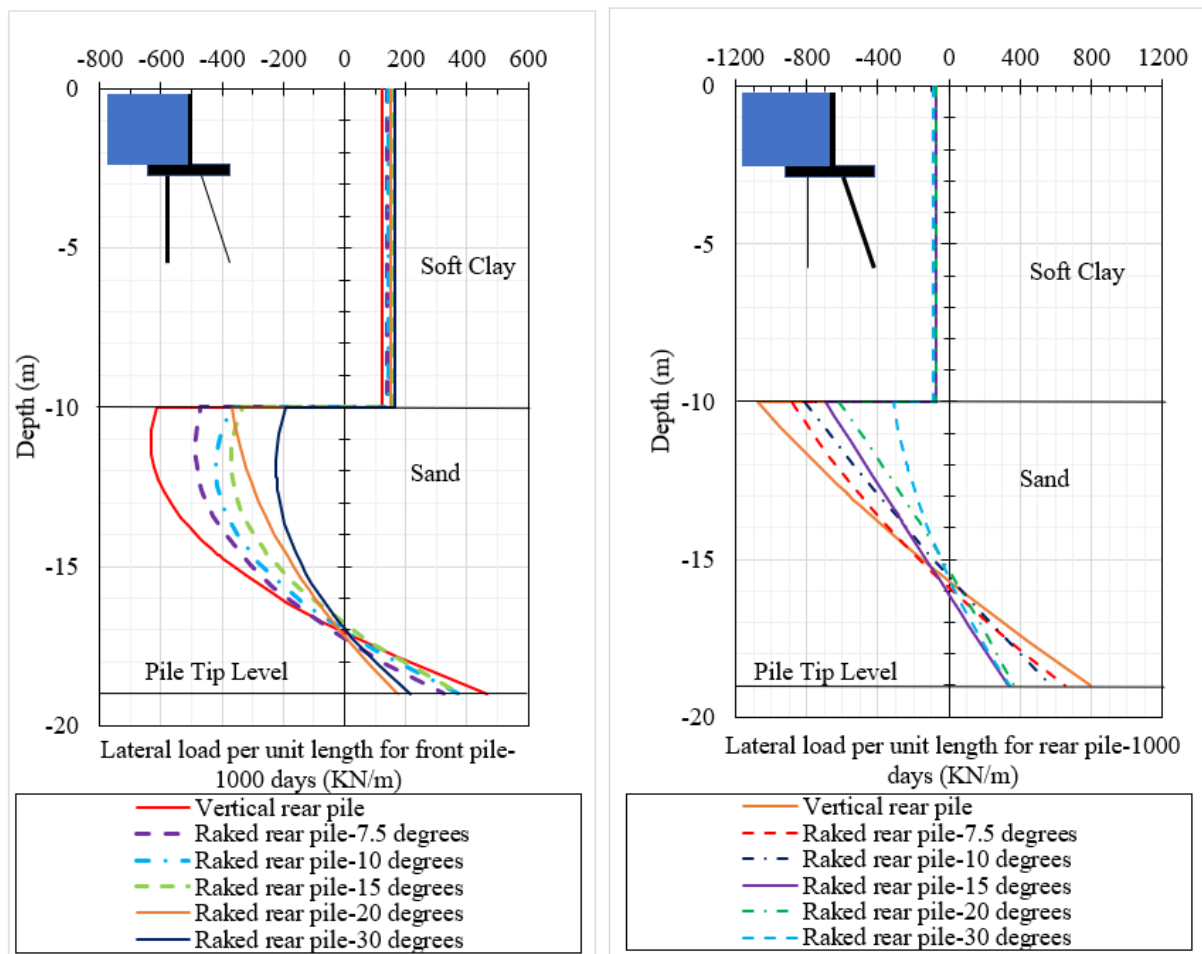


Figure 6. Lateral load per unit length for front and rear pile using different raking angles for rear pile row for 1000 days

1.2.2.3 Lateral Deformation for Front and Rear Piles

The lateral displacement of the front pile showed a decrease at both 21 days (immediately after the construction of the embankment) and 1000 days (at 90% degree of consolidation), as shown in Figures 7 and 8, respectively. At 21 days, the lateral displacement decreased by 29.10%, 36.37%, 46.71%, 53.56%, and 68.62%, and at 1000 days, it decreased by 35.56%, 38.79%, 50.61%, 57.03%, and 73.20% for rear piles with raking angles of 7.5°, 10°, 15°, 20°, and 30°, respectively, compared to the case with a vertical rear pile.

The front pile exhibited a deflected shape, increasingly pronounced with the rise in the raking angle of the rear pile, as shown in Figures 7 and 8. This deflection was a result of the increase in passive loading in the soft clay layer.

The lateral displacement of the rear pile at the head matched that of the front pile, as the pile cap is rigid, and showed the same percentage decrease in lateral displacement with increasing raking angles. However, the behavior of the rear pile differed due to the active loading, as indicated in Figure 9. Figure 10 illustrates the variations in lateral displacement at the pile head for both front and rear piles with different raking angles in the rear pile row, both at 21 days and 1000 days. The variation in lateral displacement between these two-time points decreased as the raking angle increased, suggesting that the effect of the raking degree diminished over time with the increase in raking angle.

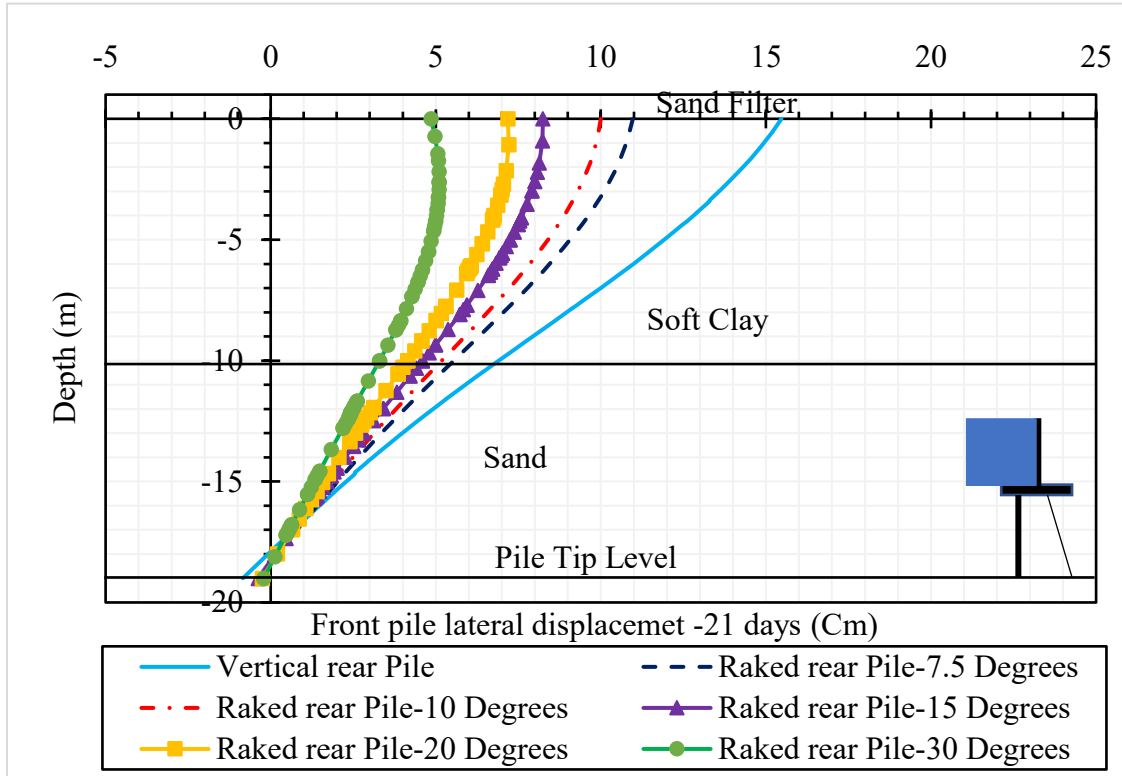


Figure 7. Lateral displacement for front pile using different raking angles for rear pile row for 21 days

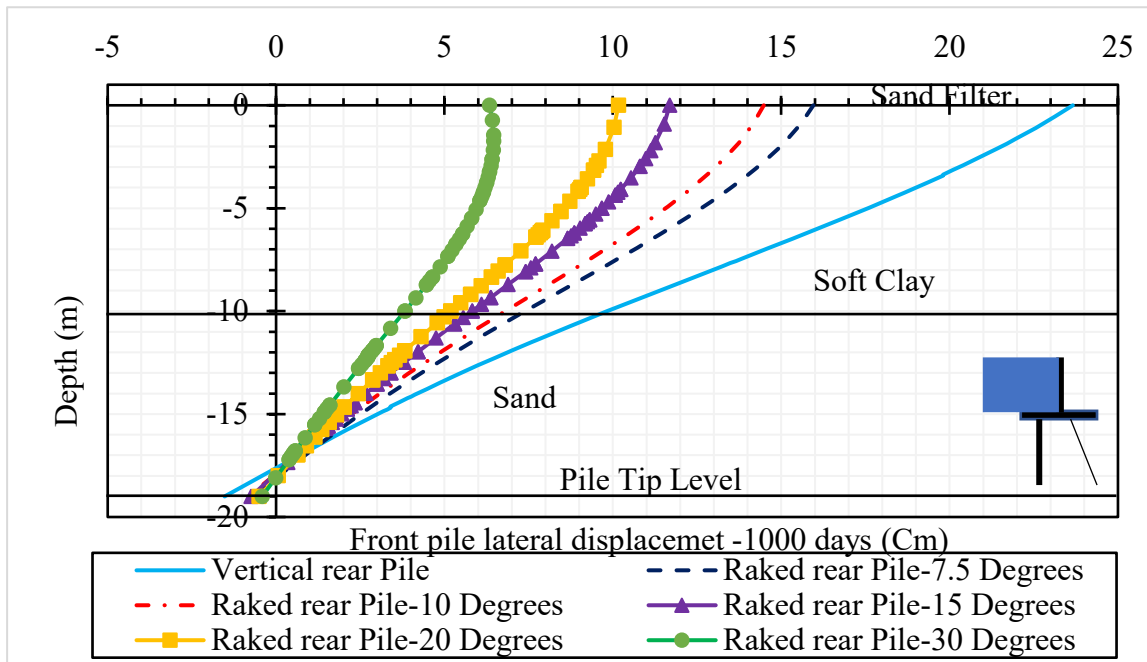


Figure 8. Lateral displacement for front pile using different raking angles for rear pile row for 1000 days.

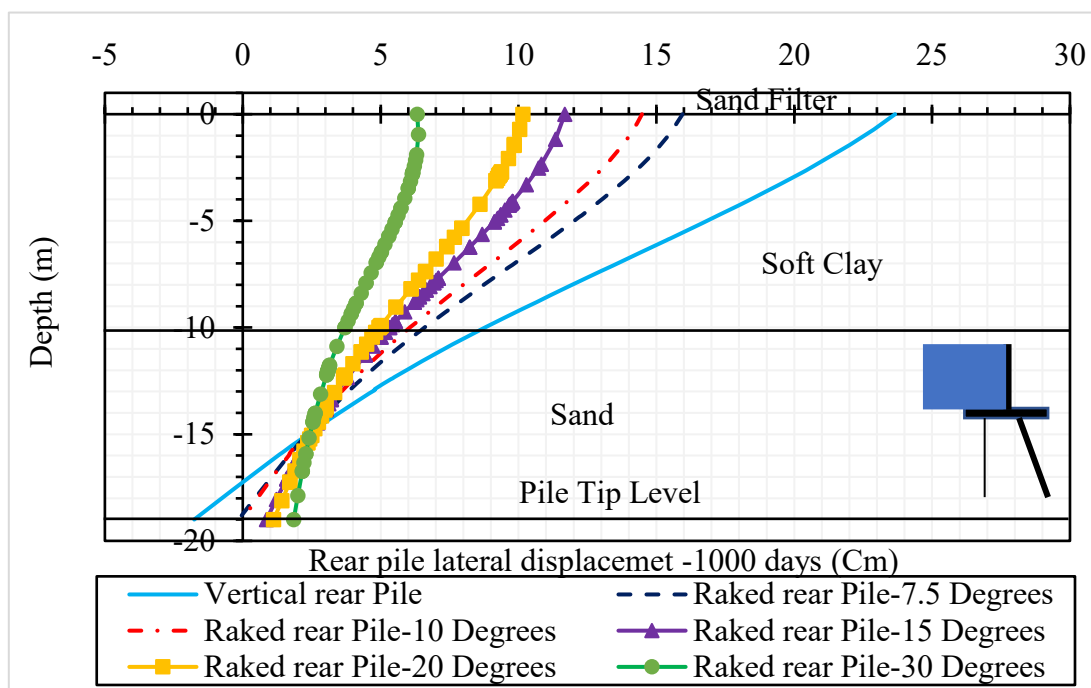


Figure 9. Lateral displacement for rear pile using different raking angles for rear pile row for 1000 days.

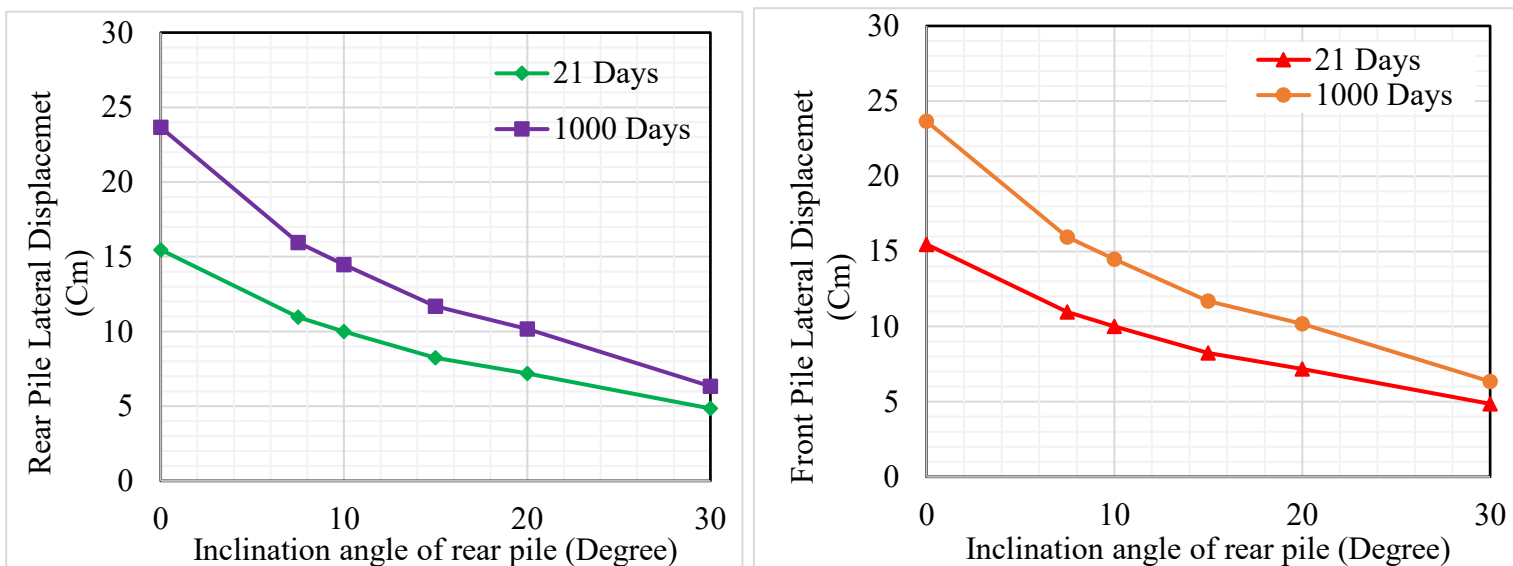


Figure 10. Variation in the lateral displacement for front and rear pile using different raking angles for rear pile row (21 days and 1000 days).

1.2.2.4 Moment for Front and Rear Pile

The bending moment at the front pile decreased as the raking angle of the rear pile increased, both at the pile head (in the positive direction) and in the negative direction, for both 21 days and 1000 days. At 21 days, the bending moment at the pile head reduced by 7.65%, 13.45%, 22.12%, 29.64%, and 45.92%, and at 1000 days, it decreased by 1.53%, 11.43%, 20.18%, 28.97%, and 44.65% for raking angles of 7.5°, 10°, 15°, 20°, and 30°, respectively, compared to a vertical rear pile. An increase in the raking angle of the rear pile altered the conflict point of the bending moment for the front pile, with the conflict point moving closer to the pile tip as the raking angle increased. For 1000 days, the conflict point was located at depths of 8.2, 9.2, 9.5, 10.0, 10.0, and 11.5m for rear pile raking angles of 0°, 7.5°, 10°, 15°, 20°, and 30°, respectively. Additionally, the location of the maximum negative moment shifted with increasing raking angle, with the maximum negative moments found at depths of 13.064, 13.113, 13.36, 13.539, 13.345, and 13.674m for the respective raking angles at 1000 days.

Similarly, for the rear pile, the bending moment at the pile head decreased with an increase in the raking angle in both the positive and negative directions at 21 days and 1000 days. The decrease in bending moment at 21 days was 1.58%, 7.76%, 14.90%, 24.87%, and 39.13%, and at 1000 days, it was 1.56%, 10.81%, 20.82%, 32.51%, and 47.48% for rear piles with raking angles of 7.5°, 10°, 15°, 20°, and 30°, respectively, compared to a vertical rear pile. At 1000 days, the conflict point of the bending moment for the rear pile in the case of a vertical rear pile was at 6.8m, and with increasing raking angle, it was approximately at 7.3m for all raking angles, with the maximum negative moment located at depths of 11.96, 12.733, 12.795, 11.681, 12.435, and 13.95m for the respective raking angles.

Figure 11 shows the variation in bending moment at the pile head for both front and rear piles with different raking angles in the rear pile row at 21 days and 1000 days. The variation between these two time points for both front and rear piles decreased as the raking angle of the rear pile increased, indicating that the effect of the raking angle reduced over time with increasing raking angle.

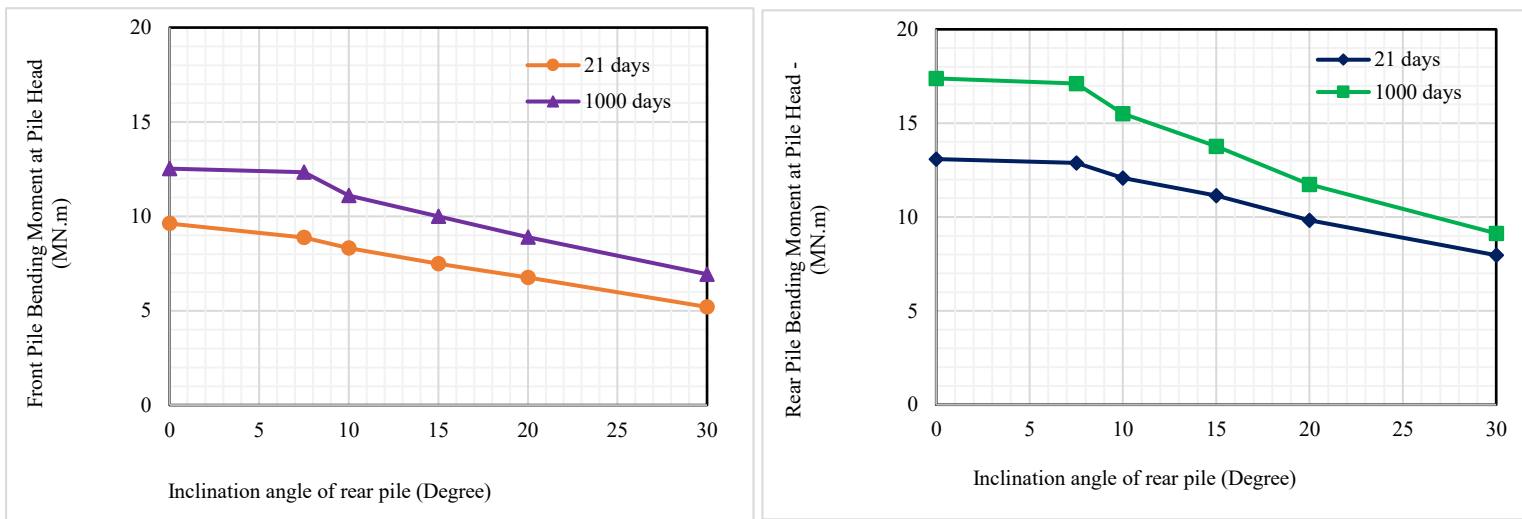


Figure 11. Variation in bending moment for front and rear pile row using different raking angles for rear pile row (21 days and 1000 days).

1.2.2.5 Shear Force for Front and Rear Pile

The shear force for front and rear piles at 1000 days. For the front pile, the shear force was observed to decrease as the raking angles increased. The trend of shear force for the front pile remained consistent across all different raking angles, except at a 30° raking angle, where the shear force did not revert to a positive value. The decrease in shear force at the pile head was 26.50%, 42.39%, 64.64%, and 75.95% for rear pile raking angles of 7.5°, 10°, 15°, and 20°, respectively, compared to a vertical rear pile. For a 30° raking angle, the shear force at the pile head was zero, beginning to increase at a depth of 1.44m. Regarding the rear pile, the shear force also decreased with an increase in raking angles. The trend was similar across different raking angles, except at a 15° raking angle, where the shear force did not revert to a positive value and was almost constant, approximately zero. The reduction in shear force at the pile head was 9.19%, 17.43%, 27.94%, 39.82%, and 55.82% for rear pile raking angles of 7.5°, 10°, 15°, 20°, and 30°, respectively, in comparison to a vertical rear pile. Overall, increasing the raking angle tended to decrease the shear force, although the behavior altered at higher raking angles (Figure 12).

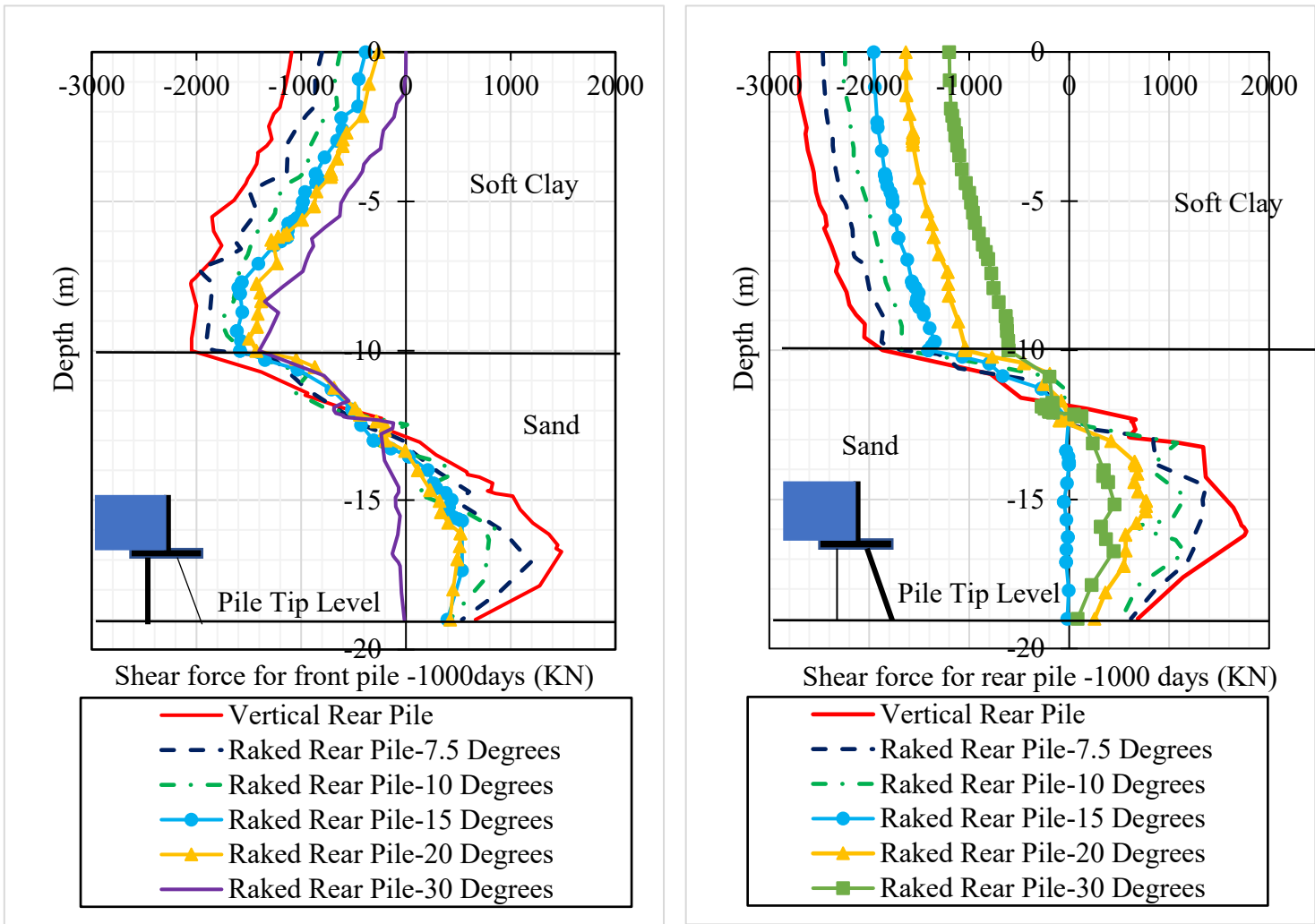


Figure 12. Shear force for front and rear pile row using different raking angle for rear pile row for (1000 days)

1.2.2.6 Deformation of the pile cap

Figure 13 illustrates the settlement of the pile cap for various raking angles in the rear pile row. In the case of the vertically piled group (VPG), the pile cap exhibited rotation away from the backfill direction. This resulted in a minor tensile (+ve) settlement for the front pile, approaching zero, and a compressive settlement (-ve) for the rear pile, leading to significant differential settlement. As the raking angle of the rear pile increased, the pile cap tended toward a more balanced position. This adjustment was marked by a decrease in settlement towards the backfill and an increase on the opposite side. At a 20-degree raking angle, the settlements on both sides were approximately equal, effectively eliminating differential settlement. Beyond this angle, the pile cap began to rotate towards the backfill direction as the raking angle of the rear pile increased further. This poses a considerable risk, as the bridge deck could potentially separate from the system.

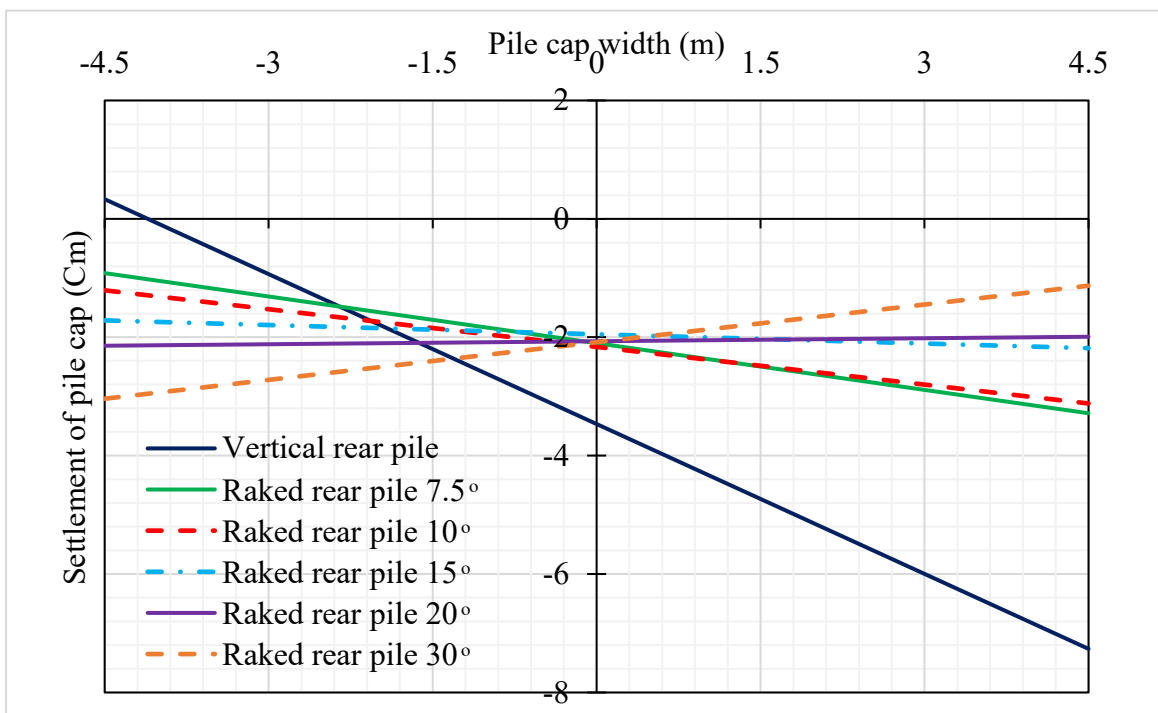


Figure 13. Settlement of pile cap using different raking angles for rear pile row for (1000 days)

1.2.2.7 Lateral deformation of the Abutment wall

The lateral movement of the abutment wall, which exhibited a behavior similar to that of the pile cap. For the vertically piled group (VPG), the movement of the abutment wall increased from the top level (8m), while the bottom level experienced less movement, equivalent to the deflection of the pile cap (Figure 14). As the raking angle of the rear pile increased, the abutment wall tended towards a balanced position. This equilibrium was nearly achieved at a 20-degree raking angle, where the lateral movements at the top and bottom levels were approximately equal. Beyond this angle, the wall began moving towards the backfill direction as the raking angle of the rear pile continued to increase. As previously mentioned, it is critically important to note that such a movement of the system away from the bridge deck poses a significant risk.

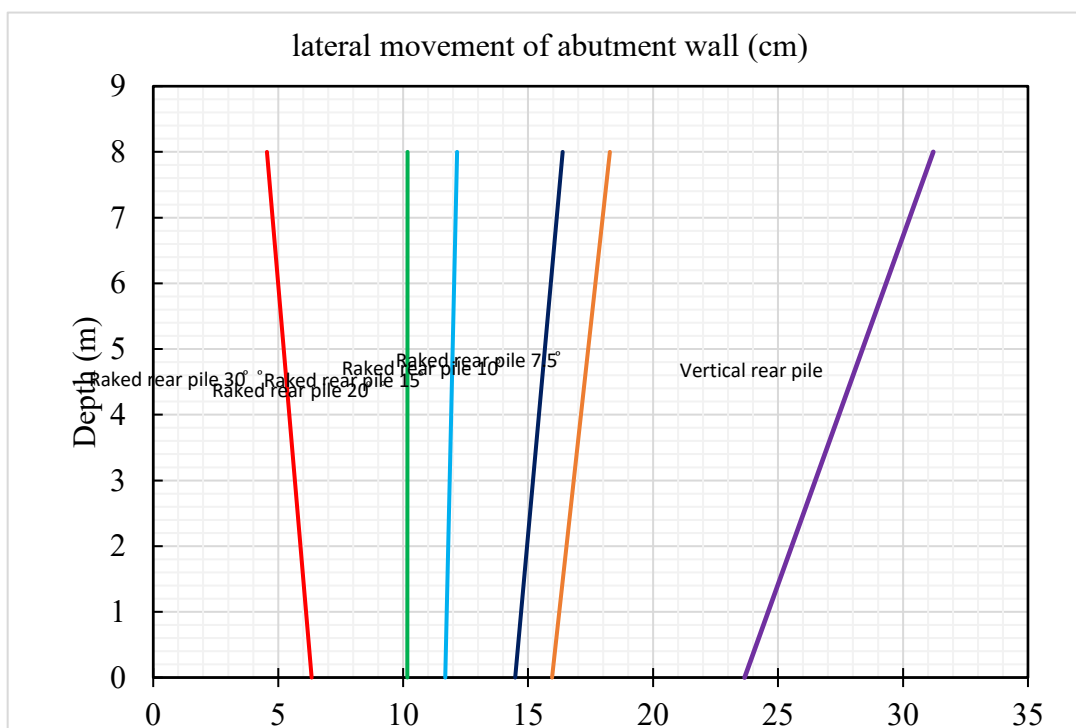


Figure 14. Lateral Movement of abutment wall using different raking angles for rear pile row for (1000 days)

1.2.2.8 Effect of Embankment Load

This impact of different embankment loads (70, 140, 245 KPa) on a pile group with varying raking angles in the rear row (0°, 10°, 20°, 30°) was examined while maintaining a constant time frame for embankment construction at 21 days. The data covers a period of 1000 days, corresponding to a 90% degree of consolidation. The embankment load values are approximately equivalent to 3, 6, and 10 times the undrained cohesion (Cu) of soft clay soil for the respective loads of 70, 140, and 245 KPa.

The lateral displacement of the front pile varies with different raking angles under varying embankment loads (Figure 15). It was observed that an increase in the embankment load led to a substantial rise in lateral displacement. In contrast, an increase in the raking angle of the rear pile was associated with a decrease in lateral displacement. The detailed outcomes of this study are compiled in Table 4.

The bending moment at the pile head of the front pile varies with different raking angles under varying embankment loads results summarized in (Figure 16)and (Table 5). For embankment loads of 70 KPa and 140 KPa, the values of bending moment decreased as the inclination angle increased. However, for an embankment load of 245 KPa, the bending moment values increased for raking angles of 10° and 20°, and then decreased for a raking angle of 30°.

The variation in lateral load per unit length for the front pile in the soft clay layer results summarized in (Figure 17)and (Table 6). Passive loading increased with higher embankment loads and with an increase in the inclination angle of the rear pile.

In the context of embankment loads, the increase in moment, lateral displacement, and lateral load can be attributed to the volumetric deformation of the soft clay layer. This deformation induces both settlement and lateral movement, subsequently exerting additional lateral pressure on the piles. As a consequence, this leads to increased bending moments and lateral displacements. Thus, when considering different raking angles, it is better to use a steeper raking angle for higher embankment loads. However, for lower embankment loads, inclining the pile may lead to damage and should be avoided.

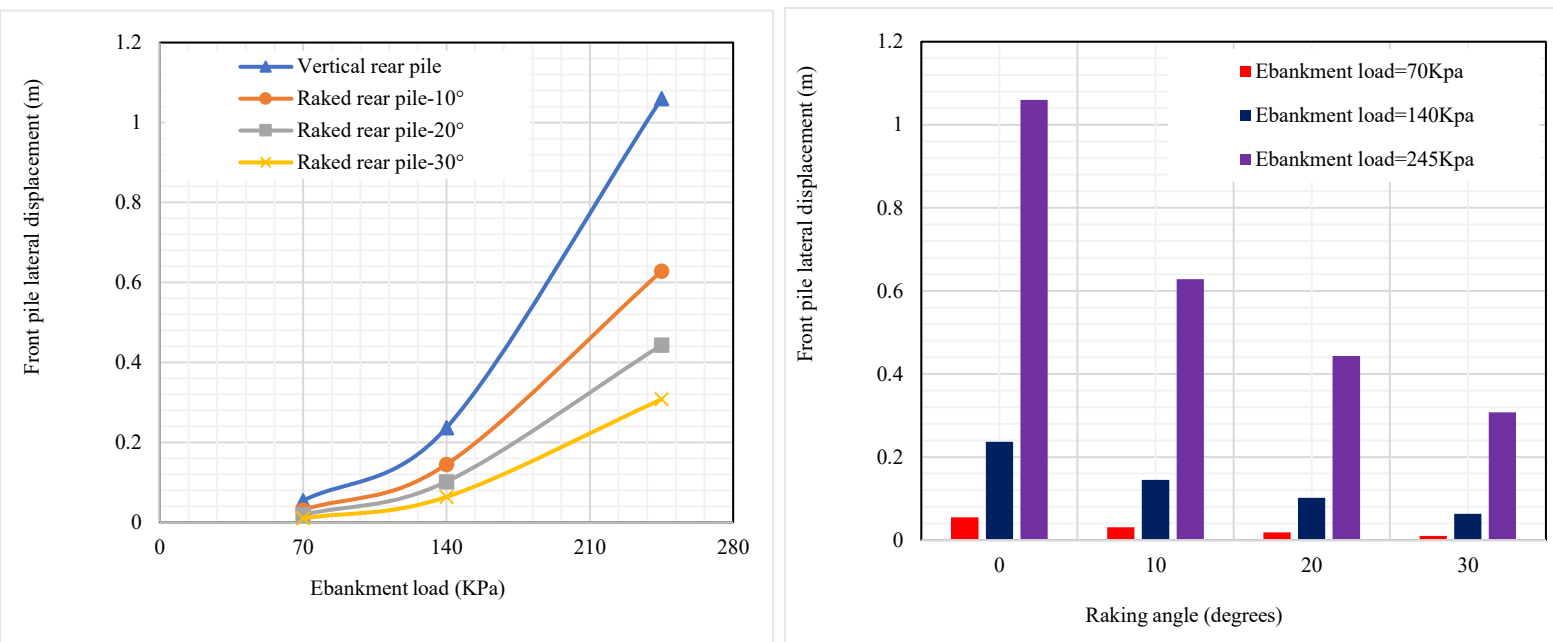


Figure 15. Variation of lateral displacement for front pile with different raking angles for rear pile using different embankment loads.

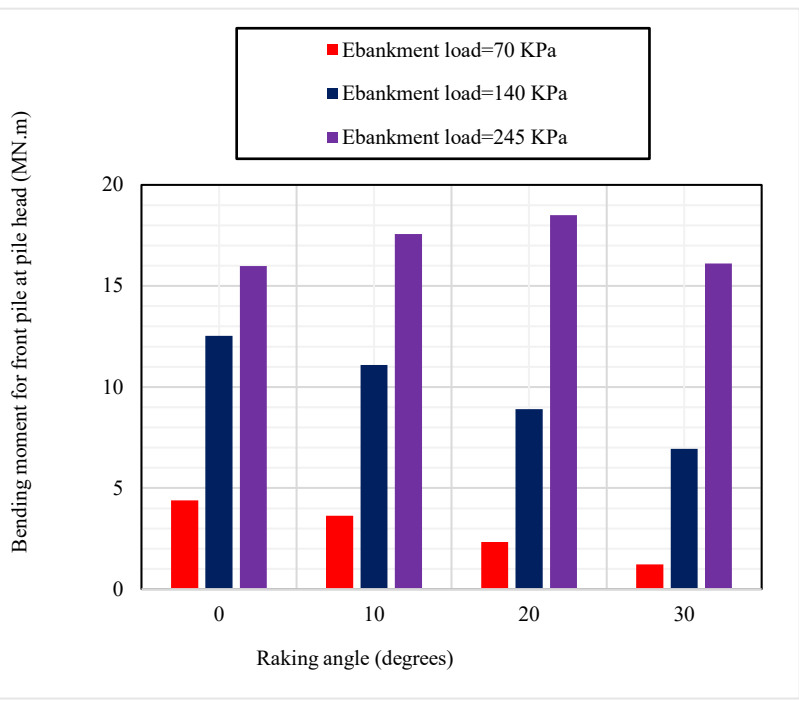
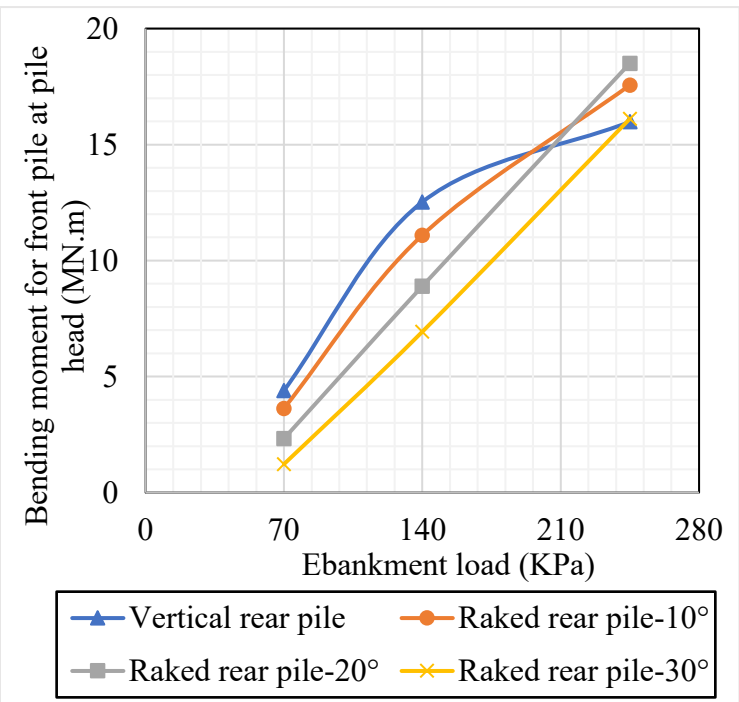


Figure 16. Variation of bending moment at pile head of front pile with different raking angles for rear pile using different embankment loads

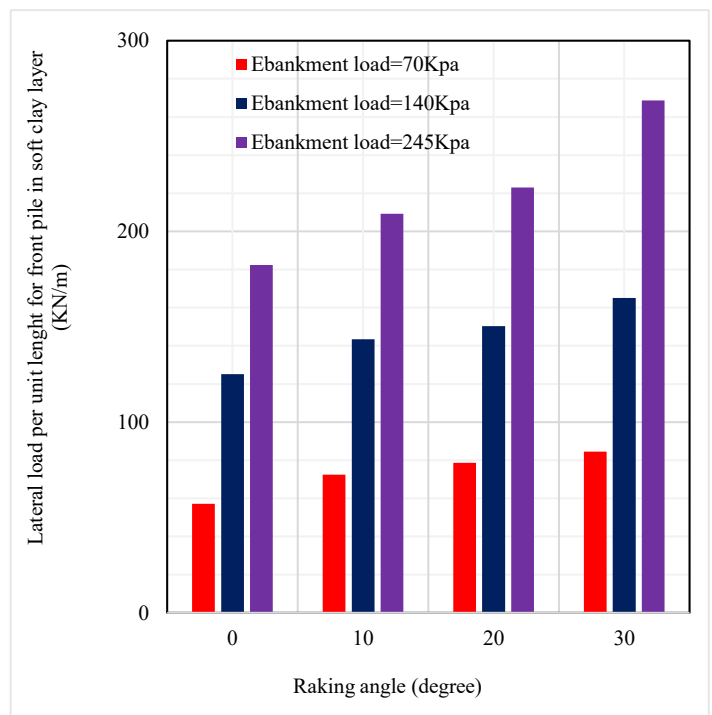
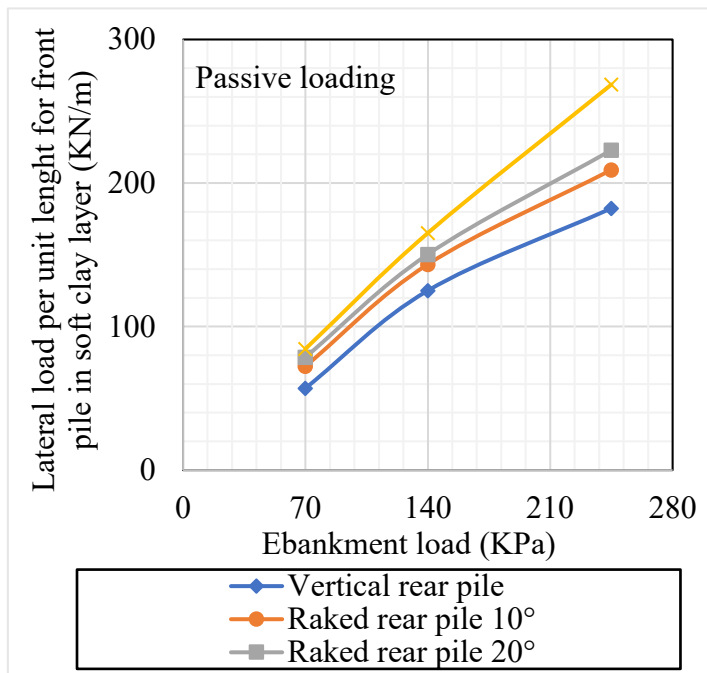


Figure 17. Variation of lateral load per unit length for soft clay layer for front pile with different raking angles for rear pile using different embankment loads

Table 4. Values of Lateral displacement for front pile using different embankment loads with different raking angles (m)

Embankment load (KPa)		70	140	245	% increase from 70KPa to 245 KPa
Raking angles (degrees)	0	0.054367	0.236612	1.059539	335, 1850
	10	0.031054	0.144835	0.628125	366, 1922
	20	0.018848	0.101673	0.443151	439, 2251
	30	0.009876	0.06341	0.307618	542, 3015
% of decrease from 0°to30°		43, 65, 82	39, 57, 73	41, 58, 71	---

Table 5. Values of Bending moment for front pile at pile head using different embankment loads with different raking angles (MN.m)

Embankment load (KPa)		70	140	245	% increase from 70KPa to 245 KPa
Raking angles (degrees)	0	4.397613	12.52629	15.98117	185, 263
	10	3.630759	11.09489	17.56417	206, 384
	20	2.327301	8.897505	18.50552	282, 695
	30	1.226826	6.933702	16.11389	465, 1214
% of variation from 0°to30°		-17, -47, -72	-11, -29, -45	10, 16, 0.83	---

Table 6. Values of lateral load per unit length for front pile for soft clay layer using different embankment loads with different raking angles (KN/m)

Embankment load (KPa)		70	140	245	% increase from 70KPa to 245 KPa
Raking angles (degrees)	0	57.094	125.064	182.404	119, 219
	10	72.386	143.394	209.18	98, 189
	20	78.7	150.334	222.94	91, 183
	30	84.478	165.162	268.62	96, 218
% of decrease from 0°to30°		27, 38, 48	15, 20, 32	15, 22, 47	---

2. CONCLUSIONS

A numerical study was conducted to investigate the effect of using a single row of raked piles (RPG) under a bridge abutment in soft clay soil and to compare it with a vertical pile group (VPG) using PLAXIS 3D (v21). The study considered different factors, including the inclination angle and embankment load. Here, we present the main findings from this study:

1. Using a row of raked piles under bridge abutments causes a reduction in the overall lateral movement of the system, bending moment, and differential settlement successively with increasing raking angle. However, it shows an increase in passive loading in the front pile and a reverse movement towards the backfill, which can cause a separation of the abutment wall from the bridge deck at higher raking angles.
2. The increase in the load of the embankment led to a significant increase in lateral displacement, bending moment, and pile pressures. Thus, using a steeper raking angle in the case of high embankment loads is recommended. Conversely, for lower embankment loads, tilting the piles may risk causing damage and is best avoided.
3. The rotation angle of 10° shows the best performance and the increase in the rotation angle may cause high deformation in the embankment and piles.

3. REFERENCES

- Abbas, J. M., Chik, Z., & Taha, M. R. (2018). Modelling and assessment of a single pile subjected to lateral load. *Studia Geotechnica et Mechanica*, 40(1), 65-78.
- Abo-Youssef, A., Morsy, M., ElAshaal, A., & ElMossallamy, Y. (2021). Numerical modelling of passive loaded pile group in multilayered soil. *Innovative Infrastructure Solutions*, 6, 1-13.
- Al-abboodi, I., & Sabbagh, T. T. (2019). Numerical modelling of passively loaded pile groups. *Geotechnical and Geological Engineering*, 37(4), 2747-2761.
- Basack, S., & Dey, S. (2012). Influence of relative pile-soil stiffness and load eccentricity on single pile response in sand under lateral cyclic loading. *Geotechnical and Geological Engineering*, 30, 737-751.
- Bellezza, I., & Caferra, L. (2018). Ultimate lateral resistance of passive piles in non-cohesive soils. *Géotechnique Letters*, 8(1), 5-12.
- Bransby, M. F., & Springman, S. M. (1996). 3-D finite element modelling of pile groups adjacent to surcharge loads. *Computers and Geotechnics*, 19(4), 301-324.
- Comodromos, E. M., & Bareka, S. V. (2005). Evaluation of negative skin friction effects in pile foundations using 3D nonlinear analysis. *Computers and Geotechnics*, 32(3), 210-221.
- Ellis, E. A. (1997). Soil-structure interaction for full-height piled bridge abutments constructed on soft clay. PhD thesis, the Univ. of Cambridge.
- Ellis, E., & Springman, S. (2001). Full-height piled bridge abutments constructed on soft clay. *Geotechnique*, 51(1), 3-14.
- El-Mossallamy, Y. M., Hefny, A. M., Demerdash, M. A., & Morsy, M. S. (2013). Numerical analysis of negative skin friction on piles in soft clay. *HBRC Journal*, 9(1), 68-76.
- Fellenius, B. H. (2006). Results from long-term measurement in piles of drag load and downdrag. *Canadian Geotechnical Journal*, 43(4), 409-430.
- Guo, W. D. (2016). Response of rigid piles during passive dragging. *International Journal for Numerical and Analytical Methods in Geomechanics*, 40(14), 1936-1967.
- Hanna, A. M., & Sharif, A. (2006). Drag force on single piles in clay subjected to surcharge loading. *International Journal of Geomechanics*, 6(2), 89-96.
- Jeong, S., Seo, D., Lee, J., & Park, J. (2004). Time-dependent behavior of pile groups by staged construction of an adjacent embankment on soft clay. *Canadian geotechnical journal*, 41(4), 644-656.
- Jones, C.A., Stewart, D.I., and Danilewicz, C.J., 2008. Bridge distress caused by approach embankment settlement. *Proceedings of the Institution of Civil Engineers-Geotechnical Engineering*, 161 (2), 63-74. doi:10.1680/ geng.2008.161.2.63.
- Kahyaoglu, M. R., Imancli, G., Ozturk, A. U., & Kayalar, A. S. (2009). Computational 3D finite element analyses of model passive piles. *Computational Materials Science*, 46(1), 193-202.
- Karim, M. R. (2013). Behaviour of piles subjected to passive subsoil movement due to embankment construction—A simplified 3D analysis. *Computers and Geotechnics*, 53, 1-8.
- Karkush, M. O., & Kareem, Z. A. (2021). Investigation the impacts of fuel oil contamination on the behaviour of passive piles group in clayey soils. *European Journal of Environmental and Civil Engineering*, 25(3), 485-501.
- Karthigeyan, S., Ramakrishna, V. V. G. S. T., & Rajagopal, K. (2007). Numerical investigation of the effect of vertical load on the lateral response of piles. *Journal of Geotechnical and Geoenvironmental Engineering*, 133(5), 512-521.
- Kelesoglu, M., & Springman, S. M. (2011). Analytical and 3D numerical modelling of full-height bridge abutments constructed on pile foundations through soft soils. *Computers and Geotechnics*, 38(8), 934-948.
- Li, H.-q., Wei, L.-m., Feng, S.-y., & Chen, Z. (2019). Behavior of piles subjected to surcharge loading in deep soft soils: Field tests. *Geotechnical and Geological Engineering*, 37, 4019-4029.
- Loganathan, N., Poulos, H. G., & Stewart, D. P. (2000). Centrifuge model testing of tunnelling-induced ground and pile deformations. *Geotechnique*, 50(3), 283-294.
- Miao, L., Goh, A., Wong, K., & Teh, C. (2006). Three-dimensional finite element analyses of passive pile behaviour. *International journal for numerical and analytical methods in geomechanics*, 30(7), 599-613.
- Morsy, M. S. (2013). Effect of downdrag on floating and end bearing piles. In *Proceedings of the 5th International Young Geotechnical Engineers' Conference* (pp. 201-204). IOS Press.
- Moulton, L.K., GangaRao, H.V.S., and Halvorsen, G.T., 1985. Tolerable movement criteria for highway bridges. Final report FHWA/RD-85/107.
- Nowak, A. S., & Iatsko, O. (2017). Revised load and resistance factors for the AASHTO LRFD Bridge Design Specifications. *PCI J*, 62(3), 46-58.
- Oteo, C. (1977). Horizontally loaded piles-deformation influence. *Proc. 9th Int. Conf. Soil Mechanics and Foundation Engineering*.
- Pan, J. L., Goh, A. T. C., Wong, K. S., & Teh, C. I. (2002). Ultimate soil pressures for piles subjected to lateral soil movements. *Journal of Geotechnical and Geoenvironmental Engineering*, 128(6), 530-535.
- Poulos, H. G. (1973). Analysis of piles in soil undergoing lateral movement. *Journal of the soil mechanics and foundations division*, 99(5), 391-406.
- Rao, S.N., Ramakrishna, V.G.S.T., and Raju, G.B., 1996. Behavior of pile-supported dolphins in marine clay under lateral loading. *Journal of Geotechnical Engineering*, 122 (8), 607-612. doi:10.1680/geot.1984.34.4.613.
- Schanz, T., Vermeer, P., & Bonnier, P. G. (1999). The hardening soil model: formulation and verification. *Beyond 2000 in computational geotechnics*, 1, 281-296.

- Soomro, M. A., Mangnejo, D. A., Bhanbhro, R., Memon, N. A., & Memon, M. A. (2019). 3D finite element analysis of pile responses to adjacent excavation in soft clay: Effects of different excavation depths systems relative to a floating pile. *Tunnelling and Underground Space Technology*, 86, 138-155.
- Springman, S. M. (1989). Lateral loading on piles due to simulated embankment construction University of Cambridge].
- Stewart, D. P. (1992). Lateral loading of piled bridge abutments due to embankment construction. Ph. D thesis, Univ. of Western Australia.
- Stewmac, A., Devata, M., & Selby, K. (1968). Unusual movements of abutments supported on end-bearing piles. *Canadian Geotechnical Journal*, 5(2), 69-79.
- Taylor, R. N. (2018). Centrifuges in modelling: principles and scale effects. In *Geotechnical centrifuge technology* (pp. 19-33). CRC Press.
- Yang, M., Shangguan, S., Li, W., & Zhu, B. (2017). Numerical study of consolidation effect on the response of passive piles adjacent to surcharge load. *International Journal of Geomechanics*, 17(11), 04017093.
- Zhang, X., Tang, L., Li, X., Ling, X., & Chan, A. (2020). Effect of the combined action of lateral load and axial load on the pile instability in liquefiable soils. *Engineering Structures*, 205, 110074.
- Zhao, M. H., Liu, D. P., Zhang, L., & Jiang, C. (2008). 3D finite element analysis on pile-soil interaction of passive pile group. *Journal of Central South University of Technology*, 15(1), 75-80.
- Zhou, D., Zhu, Q., & Wang, C. (2023). Experimental Investigation on Performances of Battered Piles Resisting Embankment-Induced Lateral Soil Movement. *Applied Sciences*, 13(18), 10333.